Improved Equivalent Circuit Model for Complementary Split Ring Resonators

Edgar Jirousek[1], Jure Soklič[2], Holger Arthaber[3]
Institute of Electrodynamics, Microwave and Circuit Engineering, TU Wien, Austria
[1,3]Christian Doppler Laboratory for Location-aware Electronic Systems
{[1]edgar.jirousek, [2]jure.soklic, [3]holger.arthaber}@tuwien.ac.at

***Abstract* — Complementary split ring resonators (CSRRs) have been used in many applications for several years, such as sensors or structures for filter-size reduction. In the literature, different equivalent circuit models for CSRRs are found. We study those approaches and analyze which circuit topology gives the highest modeling accuracy. For this purpose, we use a least squares error metric to quantify the difference between the scattering matrices (S-matrices) of different equivalent circuits and the CSRRs simulated in a 3-D full-wave simulation (FWS). To identify the best circuit topology, we consider both a wide frequency range and variations of the CSRR's size. Firstly, for each geometry, the "reference" S-matrix of the structure is found with the FWS Ansys HFSS. Secondly, the different equivalent circuits' elements are derived by means of least mean square error minimization. Plotting the resulting errors of each investigated equivalent circuit topology over the CSRR's size reveals which model performs best. As a next step, the best model is studied in detail and its circuit parameters' dependencies on the CSRR's geometry are discussed.**

***Keywords* — Split ring resonators, Equivalent circuits**

I. Introduction

Since their introduction in 2004 [1], complementary split ring resonators (CSRRs) have found many applications in the literature, including sensors for material characterization, measuring blood glucose levels, and as a tool for miniaturizing antennas on printed circuit boards (PCBs) [2]–[7]. Equivalent circuit models are a popular tool when using CSRRs, due to their significantly lower numerical complexity compared to 3-D full-wave simulations (FWSs). So far, determining the elements is done in one of two ways. One method is by using an analytical model based on the CSRR's geometry such as in [8]. The other method uses measured or simulated results of the scattering parameters (S-parameters) of a CSRR, and involves solving equations at three frequencies to determine the values for the elements in the CSRR's equivalent circuit [5], [9], [10]. The solutions of either approach are validated by comparing them to the solutions of an FWS or measurements, though only for at most a few different CSRR-sizes. How the equivalent circuit elements relate to the CSRR-size according to FWS-results over a range of CSRR-sizes is yet to be documented.

We introduce a study on equivalent circuit models for CSRRs, where microstrip-coupled rectangular CSRRs are simulated over a range of sizes using Ansys High Frequency Structure Simulator (HFSS), and the effect of the CSRR's size on every element in the equivalent circuit is discussed. Instead of relying on a few frequency points to determine the equivalent circuit's element values, we incorporate hundreds to thousands of frequency points and define the equivalent circuit elements as solutions to a least squares problem. First, we define an error metric between two scattering matrices (S-matrices), that of a HFSS-simulation and that of an equivalent circuit, using the Frobenius norm. The frequency range that the error metric takes into account spans a factor of four, with the frequency of minimum transmission of the microstrip-coupled CSRR as the geometric mean. The error metric fulfills two purposes: It serves to find optimal values for the elements in the equivalent circuits, i.e., we can determine the values for each element in an equivalent circuit by minimizing the resulting error. Further, it enables a fair comparison between different circuit models, i.e., after having optimized each element in each equivalent circuit model, better circuit models yield smaller errors. For each size of the CSRR, we use the error metric to determine the values of each element. In particular, the values for each element are found when the error is minimized. The determined values for each element in the equivalent circuit are thus the solutions to an optimization problem. We proceed to investigate the resulting errors for various CSRR-sizes and circuit models, to determine the circuit model with the lowest error. Having determined the one that approximates an FWS best, we study how each element of the equivalent circuit changes with respect to the CSRR-size. We further use the error metric to show how much the error increases after varying each circuit element, which we call an element's sensitivity.

This paper is structured as follows: In Section II, we define the equivalent circuit models, the FWS of the CSRR, and our proposed error metric. In Section III, we optimize the elements of each equivalent circuit to the FWS-results and conclude which equivalent circuit performs best. We proceed to a detailed analysis on how the equivalent circuit's elements change with respect to the CSRR's size, and which element is most sensitive to the error. This work is concluded in Section IV.

Contribution: We define the values for elements in an equivalent circuit for a CSRR as solutions to a least-squares problem, taking the complex S-matrices of an FWS and an equivalent circuit for a broad frequency range into account. The resulting mean square error enables a fair comparison between different circuit models. The equivalent circuit parameters'

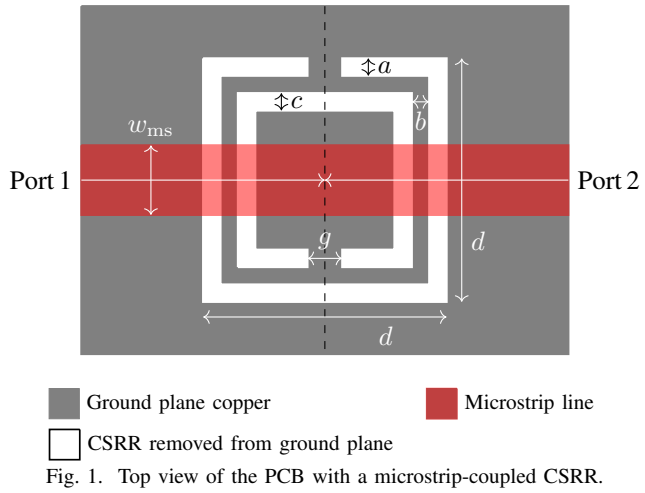

Fig. 1. Top view of the PCB with a microstrip-coupled CSRR.

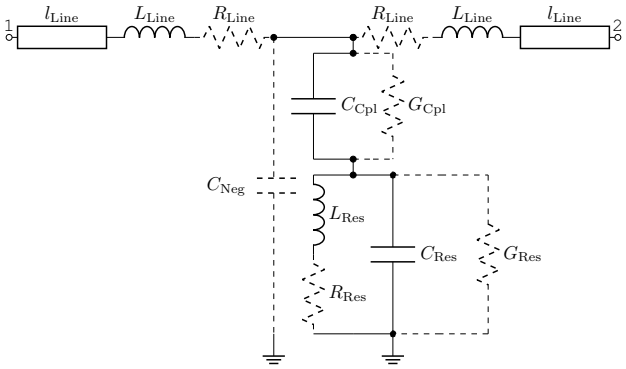

Fig. 2. Equivalent circuit for a microstrip-coupled CSRR. Dashed elements are implemented in different ways.

dependencies on the CSRR's geometry are discussed.

II. Design and Simulation

A. HFSS Simulations

Figure 1 shows the layout of the microstrip line and the CSRR on a large PCB. The dimensions from Fig. 1 are listed in Tab. 1. The substrate height and the copper thickness are $0.8\,\mathrm{mm}$ and $17\,\mu\mathrm{m}$, respectively. The substrate material is FR-4, with a relative permittivity of 4.4 and a loss tangent of 0.02.

Table 1. Dimensions of the simulated CSRR.

Property	a	b	c	d	g	w_{ms}
Length in mm	0.39	0.22	0.38	2.5–20.0	0.22	1.47

We generate the PCBs in HFSS according to the definitions in Fig. 1 and Tab. 1. Wave ports are used on each end of the microstrip line as excitations. Both ports are de-embedded to the center of the PCB, as indicated by the dashed line in Fig. 1.

B. Equivalent Circuit Models

The circuit in Fig. 2 serves as the basis for the circuit model variations that we compare. The models differ in how the dashed elements are implemented. The microstrip lines, also used in [10], have a length of l_{Line}, and are implemented according to [11]. We expect the sign of l_{Line} to be negative, given that the reference planes of both ports are at the center of the structure in the FWS. This is equivalent to shifting the reference planes apart in the FWS by $2\,|l_{\mathrm{Line}}|$ and removing the microstrip lines in the equivalent circuit. Removing all dashed elements (replacing all series resistors with a short, and shunt capacitors and resistors with an open) corresponds to the equivalent circuit proposed in [8], aside from the microstrip line. The shunt capacitor C_{Neg} is an attempt to emulate the negative permittivity for microstrip lines where CSRRs are periodically removed from the ground plane [8], [10]. The shunt resistors G_{Cpl} and G_{Res} take losses into account [6]. We further investigate the influence of the series resistors R_{Res} and R_{Line}. The following variations are studied: The elements C_{Neg}, G_{Cpl}, and G_{Res} are either allowed to have non-zero values for the capacitance and conductance, or they are replaced with an open, resulting in eight variations. The series resistors R_{Res} and R_{Line} can be implemented in three different ways: They can be replaced by a short, have a value that is constant over frequency, or they can obey the skin effect, using the relations

$$R_{\mathrm{Line}}(f) = R_{\mathrm{Line},0}\sqrt{\frac{f}{1\,\mathrm{GHz}}} \tag{1}$$

$$R_{\mathrm{Res}}(f) = R_{\mathrm{Res},0}\sqrt{\frac{f}{1\,\mathrm{GHz}}}, \tag{2}$$

resulting in 9 variations. In total, there are 72 possible circuits.

C. Optimization

The following procedure is performed independently for every value of d: The S-matrix of the HFSS-simulation $S^{(\mathrm{EM})}$ is computed over a frequency range that contains over 160 linearly spaced frequency points f_k in the interval $[f_{\mathrm{Res}}/2, 2f_{\mathrm{Res}}]$, where f_{Res} is the frequency where $\left|S_{21}^{(\mathrm{EM})}\right|$ has its first local minimum. The equivalent circuit parameters are found by minimizing the error E, defined as

$$E = \frac{1}{k_{\max} - k_{\min} + 1} \sum_{k=k_{\min}}^{k_{\max}} \left\| S^{(\mathrm{EM})}(f_k) - S^{(\mathrm{EC})}(f_k) \right\|_F^2, \tag{3}$$

where $\left|S_{21}^{(\mathrm{EC})}\right|$ is the S-matrix for the equivalent circuit, and the definitions $f_{k_{\min}} = f_{\mathrm{res}}/2$ and $f_{k_{\max}} = 2\,f_{\mathrm{res}}$ apply.

III. Results

In this section, the equivalent circuit parameters are always optimized according to the procedure described in Section II-C.

A. Equivalent Circuit Comparison

Figure 3 shows the error E for all 72 circuit variations. Eleven of these are marked and are defined in Tab. 2. The lossless models (Models 1 and 2) have the largest error (above

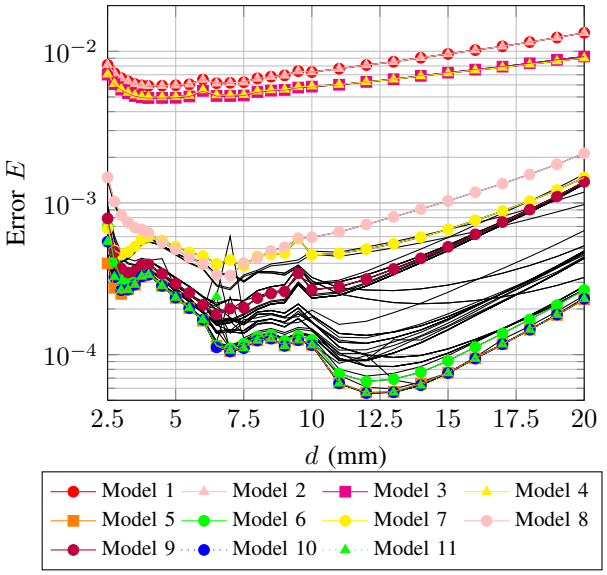

Fig. 3. Error with respect to d for all circuit models. Models from Tab. 2 are in the legend.

$4 \cdot 10^{-3}$). Adding only C_{Neg} or R_{Line} (Models 2, 3, and 4) does not significantly reduce E. Adding G_{Res}, G_{Cpl}, or R_{Res} reduces E by an order of magnitude (Models 7, 8, and 9). Using all elements and making the series resistors R_{Res} and R_{Line} obey the skin effect yields the smallest error (Model 5). However, incorporating C_{Neg} causes the system to be overdetermined and does not noticeably reduce the error. The overdetermination causes some of the circuit elements to have relations with d that follow no obvious patterns. An example is shown in Fig. 4. Furthermore, when including both R_{Res} and G_{Res} in Model 11, the optimized values for R_{Res} go to zero, except at two values for d, where the error spikes up. These are indications that Model 11 is also overdetermined. Model 10, which involves neither C_{Neg} nor R_{Res}, yields similar results as Model 5, despite lacking two degrees of freedom. In conclusion, Model 10 from Tab. 2 represents a CSRR in an FWS most accurately.

Table 2. Implementations of dashed circuit elements for selected circuit models highlighted in Fig. 3.

Model	C_{Neg}	G_{Cpl}	G_{Res}	R_{Line}	R_{Res}
Model 1	open	open	open	short	short
Model 2	$<0\,\mathrm{F}$	open	open	short	short
Model 3	open	open	open	const. over f	short
Model 4	open	open	open	$\propto \sqrt{f}$	short
Model 5	$<0\,\mathrm{F}$	$>0\,\mathrm{S}$	$>0\,\mathrm{S}$	$\propto \sqrt{f}$	$\propto \sqrt{f}$
Model 6	open	$>0\,\mathrm{S}$	open	$\propto \sqrt{f}$	$\propto \sqrt{f}$
Model 7	open	open	$>0\,\mathrm{S}$	short	short
Model 8	open	$>0\,\mathrm{S}$	open	short	short
Model 9	open	open	open	short	const. over f
Model 10	open	$>0\,\mathrm{S}$	$>0\,\mathrm{S}$	$\propto \sqrt{f}$	short
Model 11	open	$>0\,\mathrm{S}$	$>0\,\mathrm{S}$	$\propto \sqrt{f}$	$\propto \sqrt{f}$

B. Optimal Equivalent Circuit

In this subsection, model 10 from Tab. 2 is studied in more detail. The results for l_{Line} are shown in Fig. 5. The negative

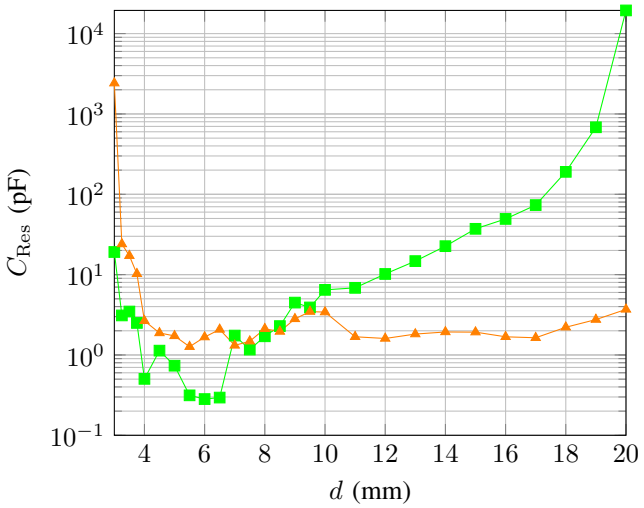

Fig. 4. Examples for values of C_{Res} with respect to d for some models that involve C_{Neg}.

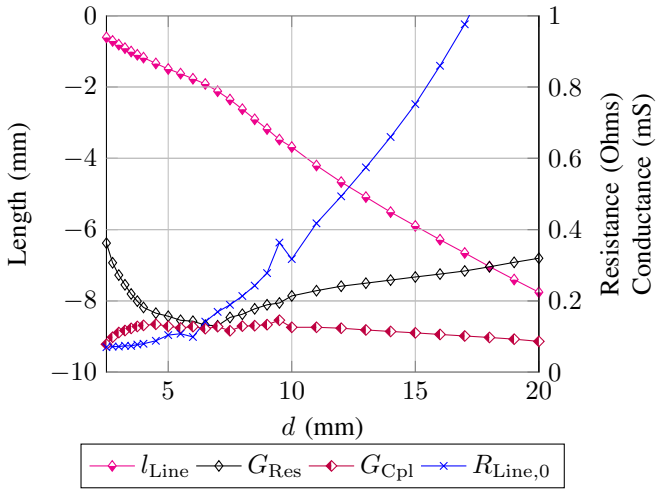

Fig. 5. Length of the microstrip line with respect to d.

sign for l_{Line} means that the CSRR acts as a lumped element with a length of $2\,|l_{\mathrm{Line}}|$. The monotonic increase of $|l_{\mathrm{Line}}|$ with d is consistent with the growing length of the CSRR parallel to the microstrip line. The results for C_{Line}, C_{Cpl}, L_{Line}, and L_{Res} are shown in Fig. 6. The values for C_{Line} and L_{Line} grow approximately linearly with d. The same can be said for L_{Res}, C_{Res}, and $|l_{\mathrm{Line}}|$ except for the interval between approximately $3\,\mathrm{mm}$ and $10\,\mathrm{mm}$. In this region, the quality factor Q of the unloaded resonator, which consists only of L_{Res}, C_{Res}, and G_{Res}, reaches a peak of 51 at $d = 7\,\mathrm{mm}$. By comparison, an eigenmode simulation in HFSS of the same PCB without the microstrip line yields $Q = 55$, with conductor losses considered.

We further investigate how E responds to a change to each parameter from the equivalent circuit. For each parameter p of the equivalent circuit, we define the sensitivity $s\,(p)$ as

$$s\,(p) = \frac{E_p - E}{E \cdot \frac{\Delta p}{p}}, \tag{4}$$

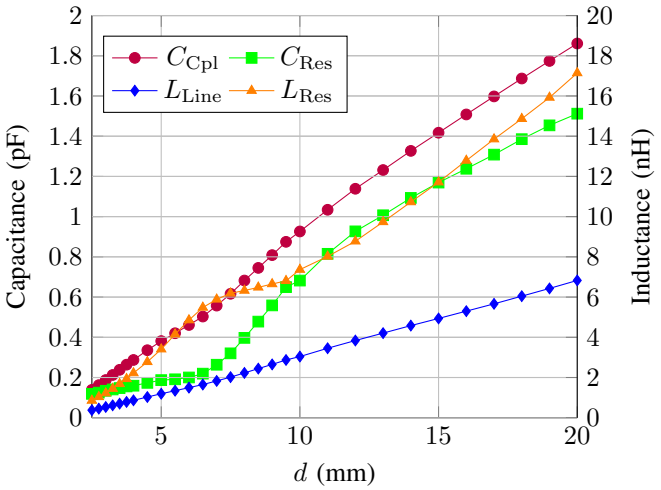

Fig. 6. Values for C_{Cpl}, C_{Res}, L_{Line}, L_{Res} with respect to d.

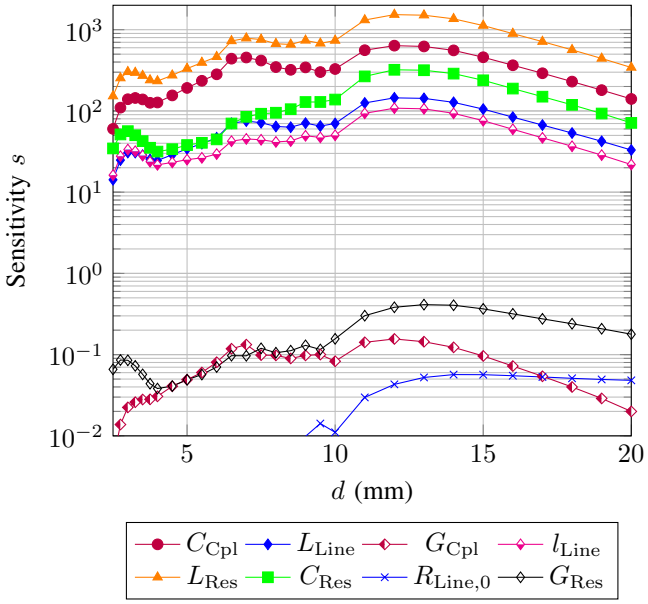

Fig. 7. Sensitivities $s\,(p)$ with respect to d, where p is one of the parameters from the legend.

where E_p is the error from (3), when the parameter p is substituted by $p + \Delta p$. The values for $s\,(p)$ are shown in Fig. 7 for $\Delta p = 0.01\,p$. The results show that the error is most sensitive towards L_{Res}, and that $s\,(L_{\mathrm{Res}})$ is four to ten times greater than $s\,(C_{\mathrm{Res}})$. Furthermore $s\,(C_{\mathrm{Cpl}}) > s\,(C_{\mathrm{Res}})$ means that the coupling effect from the microstrip line has a greater impact on E than the CSRR's capacitance C_{Res}. This implies that $s\,(C_{\mathrm{Cpl}})$ and $s\,(C_{\mathrm{Res}})$ should be optimized jointly.

IV. Conclusion

We propose a method to use S-matrices and least squares to fit equivalent circuits' parameters to FWS-results for microstrip-coupled CSRRs. We provide a study that takes FWS-results from an unprecedented range of CSRR-sizes into account, lets us conclude on the validity of using each element in the equivalent circuit, and shows the dependence of each element with respect to d. Monotonic behavior of most circuit elements with respect to d is observed. Including the resistors G_{Cpl}, G_{Res}, and R_{Line} reduces the mean square error by up to two orders of magnitude compared to a lossless model. Implementing the series resistance R_{Line} to obey the skin effect yields a smaller error compared to a resistance that is constant over frequency. The greater sensitivity of C_{Cpl} towards E than C_{Res} underlines the importance of optimizing C_{Cpl} and C_{Res} jointly rather than independently. Reducing the mean square error is better achieved by including a series resistance R_{Line} that obeys the skin effect, than with a shunt capacitance C_{Neg}. The latter causes the circuit model to be overdetermined, and can be omitted without losing accuracy.

Acknowledgment

The financial support by the Christian Doppler Research Association and the Austrian Federal Ministry for Digital and Economic Affairs is gratefully acknowledged.

References

[1] F. Falcone, T. Lopetegi, J. Baena, R. Marques, F. Martin, and M. Sorolla, "Effective negative-/spl epsiv/ stopband microstrip lines based on complementary split ring resonators," *IEEE Microwave and Wireless Components Letters*, vol. 14, no. 6, pp. 280–282, 2004.

[2] M. S. Boybay and O. M. Ramahi, "Material characterization using complementary split-ring resonators," *IEEE Transactions on Instrumentation and Measurement*, vol. 61, no. 11, pp. 3039–3046, 2012.

[3] C.-S. Lee and C.-L. Yang, "Thickness and permittivity measurement in multi-layered dielectric structures using complementary split-ring resonators," *IEEE Sensors Journal*, vol. 14, no. 3, pp. 695–700, 2014.

[4] N. K. Tiwari, P. K. Varshney, S. P. Singh, and M. J. Akhtar, "Shape perturbed tunable planar rf resonator for the dielectric measurement in wide frequency range," in *2019 8th Asia-Pacific Conference on Antennas and Propagation (APCAP)*, 2019, pp. 666–667.

[5] M. A. H. Ansari, A. K. Jha, Z. Akhter, and M. J. Akhtar, "Multi-band rf planar sensor using complementary split ring resonator for testing of dielectric materials," *IEEE Sensors Journal*, vol. 18, no. 16, pp. 6596–6606, 2018.

[6] A. E. Omer, G. Shaker, S. Safavi-Naeini, H. Kokabi, G. Alquié, F. Deshours, and R. M. Shubair, "Low-cost portable microwave sensor for non-invasive monitoring of blood glucose level: novel design utilizing a four-cell csrr hexagonal configuration," *Nature Scientific Reports*, vol. 10, no. 15200, 2020.

[7] R. k. Baee, G. Dadashzadeh, and F. G. Kharakhili, "Using of csrr and its equivalent circuit model in size reduction of microstrip antenna," in *2007 Asia-Pacific Microwave Conference*, 2007, pp. 1–4.

[8] J. Baena, J. Bonache, F. Martin, R. Sillero, F. Falcone, T. Lopetegi, M. Laso, J. Garcia-Garcia, I. Gil, M. Portillo, and M. Sorolla, "Equivalent-circuit models for split-ring resonators and complementary split-ring resonators coupled to planar transmission lines," *IEEE Transactions on Microwave Theory and Techniques*, vol. 53, no. 4, pp. 1451–1461, 2005.

[9] J. Bonache, M. Gil, I. Gil, J. Garcia-Garcia, and F. Martin, "On the electrical characteristics of complementary metamaterial resonators," *IEEE Microwave and Wireless Components Letters*, vol. 16, no. 10, pp. 543–545, 2006.

[10] C. Li, K. Liu, and F. Li, "An equivalent circuit for the complementary split ring resonators (csrrs) with application to highpass filters," in *2006 International Symposium on Biophotonics, Nanophotonics and Metamaterials*, 2006, pp. 478–479.

[11] E. Hammerstad and O. Jensen, "Accurate models for microstrip computer-aided design," in *1980 IEEE MTT-S International Microwave symposium Digest*, 1980, pp. 407–409.